Published in final edited form as:
Pharmacogenet Genomics. 2009 December ; 19(12): 923–934. doi:10.1097/FPC.0b013e3283330767.

Human UDP-glucuronosyltransferase UGT2A2: cDNA construction, expression, and functional characterization in comparison with UGT2A1 and UGT2A3

Nina Sneitz[a,b], **Michael H. Court**[c], **Xiuling Zhang**[d], **Kaisa Laajanen**[a,1], **Karen K. Yee**[e], **Pamela Dalton**[e], **Xinxin Ding**[d], and **Moshe Finel**[a]

[a] Centre for Drug Research, University of Helsinki, Finland [b] Division of Pharmaceutical Chemistry Faculty of Pharmacy, University of Helsinki, Finland [c] Comparative and Molecular Pharmacogenomics Laboratory, Department of Pharmacology and Experimental Therapeutics, Tufts University School of Medicine, Boston, Massachusetts, USA [d] Wadsworth Center, New York State Department of Health, Albany, New York, USA [e] Monell Chemical Senses Center, Philadelphia, Pennsylvania, USA

Abstract

Objectives—Characterize the expression and glucuronidation activities of the human UDP-glucuronosyltransferase (UGT) 2A2.

Methods—UGT2A1 was cloned from nasal mucosa mRNA. Synthetic cDNA for UGT2A2 was constructed assuming exon sharing between UGT2A1 and UGT2A2 (Mackenzie et al., Pharmacogenetics and Genomics 2005, 15:677–685). Exon 1 of UGT2A2 was amplified from genomic DNA and combined with exons 2–6 of UGT2A1. UGT2A3 was cloned from liver mRNA. Quantitative RT-PCR was used to evaluate the expression of all the three UGTs of subfamily 2A in different tissues. Recombinant UGT2A1, UGT2A2 and UGT2A3 were expressed in baculovirus-infected insect cells and analyzed for glucuronidation activity towards different substrates.

Results—DNA sequencing of reverse-transcribed PCR (RT-PCR) products from human nasal mucosa mRNA, confirmed exon sharing between UGT2A1 and UGT2A2. In addition, it indicated that the N-terminal signal peptide sequence of UGT2A2 is the longest among the human UGTs. Quantitative RT-PCR revealed that both UGT2A1 and UGT2A2 are mainly expressed in the nasal mucosa, and that their expression level in fetal samples was much higher than in adults. Activity assays with recombinant UGTs 2A1–2A3 demonstrated broad substrate selectivity for UGT2A1 and UGT2A2. While glucuronidation rates and substrate affinities were mostly higher in UGT2A1, the K_m values for UDP-glucuronic acid were similar in both UGTs. In addition, there were regioselectivity differences between the two UGTs and, with a few substrates, particularly ethinylestradiol, the activity of UGT2A2 was higher.

Conclusions—UGT2A2 is mainly expressed in the nasal mucosa and it has glucuronidation activity towards several different endo- and xenobiotic substrates.

Please address correspondence to Moshe Finel, CDR, Faculty of Pharmacy, P.O. Box 56 (Viikinkaari 5), FIN-00014 University of Helsinki, Finland Tel. +358 9 191 59193, Fax +358 9 191 59556, moshe.finel@helsinki.fi.
[1]Present address (K.L.): Genome-Scale Biology Program, Institute of Biomedicine, Biomedicum Helsinki, P.O. Box 63, 00014 University of Helsinki, Finland.

Keywords

Subfamily UGT2A; glucuronidation; nasal mucosa mRNA

Introduction

UDP-glucuronosyltransferases (UGTs) catalyze the conjugation of many endogenous and xenobiotic compounds with glucuronic acid from UDP-glucuronic acid (UDPGA). This glucuronidation reaction increases the water solubility of the aglycones, accelerates their excretion from the body through bile or urine, and in most cases, but not all, renders them biologically inactive (Tukey and Strassburg, 2000; King et al., 2000; Ouzzine et al., 2003; Wells et al., 2004).

The UGTs are membrane proteins of the endoplasmic reticulum that are expressed in a tissue specific manner. The liver is the main site of glucuronidation in our body and most of the UGTs are expressed in hepatocytes. Many liver UGTs are also expressed in other tissues, including intestine, kidneys, breast, placenta, testis and prostate (Belanger et al., 1998; Tukey and Strassburg, 2000; King et al., 2000; Wells et al., 2004; Nakamura et al., 2008; Ohno and Nakajin, 2009). In addition, there are several UGTs that are largely or only expressed in extra-hepatic tissues, such as different segments of the gastrointestinal tracts, lungs and nasal epithelium. The human genome contains 19 UGTs that are divided into 3 subfamilies, 1A, 2A and 2B (Mackenzie et al., 2005). In addition, the human genome contains 3 proteins that are more distantly related to the 19 UGTs of subfamilies 1 and 2, namely the UDP galactose:ceramide galactosyltransferase UGT8A1 (Mackenzie et al., 2005) and the UDP N-acetylglucosaminyltransferase UGT3A1 and UGT3A2 (Mackenzie et al., 2009). The latter proteins will not be further discussed here.

The human UGTs of subfamilies 1A and 2B have been studied extensively. Much less is known about the 3 members of subfamily 2A, the subject of this study. Only one major work on UGT2A1 (olfactory UGT) was published in the past, demonstrating, among other things, that this enzyme is mainly expressed in the nasal epithelium (Jedlitschky et al., 1999). UGT2A1 mRNA has later been found also in the human lung (Thum et al., 2006; Somers et al., 2007). Expression of the human UGT2A2 in segments of the intestinal tract, particularly duodenum and jejunum, was reported in an early study with limited experimental details (Fig. 4 in Tukey and Strassburg, 2001). Unfortunately, it remained unclear if these researchers have cloned full-length UGT2A2 mRNA since only results for exon 1 are presented in that publication. We have recently described the expression of UGT2A3, polymorphism in this enzyme, and its relatively limited activity (Court et al., 2008). In other animals, UGT2A1 mRNA has been detected in the nasal epithelium of rat and mouse (Heydel et al., 2001) while UGT2A2 mRNA was detected in the olfactory epithelium of neonatal mouse (Strausberg et al., 2002; Buckley and Klaassen, 2007). It may be noted, however, that in the study of Buckley and Klaassen (2007) there was no attempt to distinguish between the expression of UGT2A1 and UGT2A2 in the mouse nasal epithelia. In the same study, UGT2A3 was found to be highly expressed in the mouse liver, and it was also found in the mouse gastrointestinal tract (Buckley and Klaassen, 2007).

The C-terminal half of all the UGTs is highly conserved and among the 9 members of subfamily UGT1A the primary structure of this domain is identical due to exon sharing (Mackenzie et al., 2005; Owens et al., 2005; Gong et al., 2001). Exon sharing between UGTs 2A1 and 2A2 was also suggested (Mackenzie et al., 2005), but not yet demonstrated. In UGT2A3 and in all the 7 members of subfamily 2B there is no exon sharing. Their C-

terminal halves are nevertheless highly similar to each other, as well as to the corresponding domains in UGT1As and UGT2A1 (Mackenzie et al., 2005).

The substrate selectivityof the UGTs is complex, and most of the UGTs can glucuronidate several different compounds that vary significantly in their chemical structure. On the other hand, there are human UGTs that so far show only minimal activity for certain substrates, such as UGT2B11 (Turgeon et al., 2003), or a very limited substrate selectivity such as UGT2A3 (Court et al., 2008). Interestingly, subfamily 2A of the human UGTs includes both an enzyme with exceptionally broad substrate selectivity, UGT2A1 (Jedlitschky et al., 1999; Sten et al., 2009), and an enzyme with a highly restricted substrate selectivity, UGT2A3 (Court et al., 2008). It is thus very interesting to examine the activity of the human UGT2A2, the 3rd and last member of this subfamily, with a collection of different substrates in order to try and “map” the differences in activities and substrate affinities among this least studied subfamily of human UGTs.

Materials and Methods

Materials

Bovine serum albumin (essentially fatty acid free), 4-aminobiphenyl, B-estradiol, β-estriol, 17α-ethinylestradiol, 1-hydroxypyrene, hyodeoxycholic acid (HDCA), 4-methylumbelliferone α-naphthol, 4-nitrophenol, umbelliferone, uridine 5′-diphosphoglucuronic acid triammonium salt, and D-saccharic acid 1, 4-lactone were purchased from Sigma-Aldrich (St. Louis, MO, USA.). 4-hydroxybiphenyl and 2-hydroxybiphenyl were from Fluka (Germany), whereas 3-hydroxybiphenyl was from Chiron (Trondheim, Norway).β-estradiol 3-(β-D-glucuronide) sodium salt, β-estradiol 17-(β-D-glucuronide) sodium salt, estriol 16α-β-D-glucuronide, estriol 3-β-D-glucuronide, 4-methylumbelliferyl β-D-glucuronide, α-naphthyl β-D-glucuronide, 4-nitrophenyl β-D-glucuronide and umbelliferyl β-D-glucuronides were from Sigma-Aldrich. The 7-Hydroxycoumarin β-D-glucuronide was purchased from Ultrafine Synergy-House (Manchester, UK), whereas 1-hydroxypyrene glucuronide was synthesized in our lab as previously described (Luukkanen et. al. 2001). Radiolabeled[^{14}C] UDPGA was purchased from PerkinElmer Life and Analytical Sciences (Boston, MA).

Cloning and expression of UGT2As

The Institutional Review Board at the New York State Department of Health approved the study. Total RNA was prepared using TRIzol reagent (Invitrogen, Carlsbad, CA), as described previously (Zhang et al., 2005). Nasal tissue from a male African American fetus (gestational age of 91 days) was provided by the University of Washington Birth Defects Research Laboratory. Following DNAse treatment, reverse transcription was performed using the SuperScript III First-Strand Synthesis System (Invitrogen). The UGT2A1 cDNA was amplified by high-fidelity PCR, with use of the Pfx50 DNA polymerase (Invitrogen), and using 5′-CTT CTG CAT CAA GCC ACA TCA TGT-3′ and 5′-CTA CTC AGG ATT TTG CCA AAC TTA AGA-3′ as the forward (sense) and reverse (anti-sense) primers, respectively. The PCR product was subsequently cloned into the PCR-Script vector (Agilent Technologies, La Jolla, CA), and sequenced in both directions using primers F1 (5′-CCA CCT ACA GGA CTA CAT G-3′), F2 (5′-TTA CCA CGG AGT CCC TAT G-3′), R1 (5′-CCA TGT CGA AAC GAA GTC CT-3′), and R2 (5′-AGT CTC ACA TAA CGT AGT GG-3′). Differences between the cloned cDNA sequence and the previously published UGT2A1 mRNA sequence are described in the Results section. UGT2A3 was cloned from liver mRNA, as described recently (Court et al., 2008).

UGT2A2 cDNA was constructed by cloning exon 1 of UGT2A2 from human genomic DNA and ligating it to exons 2–6 of UGT2A1. To this end, a new Aat2 restriction site was created by a silent mutation just downstream of the expected junction point between exons 1 and 2 of UGT2A2. This new site was included (underlined) in the anti-sense oligo that was designed to amplify exon 1 of UGT2A2 from human genomic DNA, 5′-AGG ACG TCC TAA AAT TTT GCT ATA GTA TGA ATT C-3′, as well as in the sense oligo that was designed to amplify exons 2–6 of UGT2A1 from the cloned cDNA in PCR-Script, 5′-AGG ACG TCC CAC TAC GTT ATG TGA GAC TA-3′. The sense oligo for the amplification of exon 1 of UGT2A2, 5′-AGG ATC CTA CAG TAG GAT GGT TTC CAT AAG-3′, contained an upstream BamH1 restriction site (underlined) to facilitate subcloning into the shuttle vector FB-XHA (Kurkela et al., 2003), a derivative of pFastBac (Invitrogen, Carlsbad, CA, USA). To generate His-tagged UGT2A1 and UGT2A2, the stop codon in exon 6 of UGT2A1 was replaced by a Sal1 restriction site, in frame with the C-terminal fusion peptide in FB-XHA (Kurkela et al., 2003). This was done using the following oligonucleotide, 5′-TTG GTC GAC TCT CTT TTT TTC TTC TTT CCT ATC-3′ (the Sal1 restriction site is underlined), as the anti-sense primer for the amplification of exons 2–6 of UGT2A1. A corresponding manipulation was done for UGT2A3, namely an insertion of a BamH1 restriction site upstream the first ATG, and a Sal1 restriction site that replaces the endogenous stop codon, using the respective oligonucleotides 5′-AGG GAT CCG CCA TCA TGA GGT CTG A-3′ and 5′-AAG GTC GAC TCC CTC TTT TCT ATC TTT C-3′.

Recombinant UGTs 2A1–2A3, all with C-terminal His tags, were expressed in baculovirus-infected insect cells as previously described (Kurkela et al., 2003). Membranes (microsomes) were collected from the harvested cells, and protein concentrations were measured by the bicinchoninic acid method (Pierce, Rockford, IL, U.S.A.), using bovine serum albumin as a standard. The relative expression levels of the recombinant UGTs, all of which carry a C-terminal His-tag, was determined using the monoclonal anti-His-tag antibodies tetra-His (Qiagen, Hilden, Germany), as previously described (Kurkela et al., 2004 and 2007).

Screening of human tissues for UGT2A2 mRNA expression

Total RNA from human fetal nasal mucosa (2 individuals), fetal lung (2 individuals), adult lung (3 individuals, 32–61 year old male and two females Caucasians), fetal liver (2 individuals and a pooled sample) and adult liver (pooled) were screened for UGT2A2 mRNA expression by RT-PCR. Individual fetal tissues (provided by the University of Washington Birth Defects Research Laboratory) were from two female fetuses, one Alaskan native (#1), the other Caucasian (#2), both with a gestational age of 103 days. Pooled fetal liver total RNA (n =63 white American donors) were from BD-Clontech (USA), while pooled adult liver RNA (n = 47 white American donors) were extracted using Trizol reagent from liver bank samples (Department of Pharmacology and Experimental Therapeutics, Tufts University School of Medicine, Boston, MA). Use of the adult liver tissues was approved by the institutional review board of Tufts University School of Medicine. Following DNase treatment and reverse transcription, PCR was performed using Platinum HiFi Supermix (Invitrogen), including 1 μL of 1:10 diluted cDNA and 200 nM of each primer. Primer pair sequences were as follows: 5′-GAC CAG ATG ACC TTT GGT GAA AGG ATT-3′ (UGT2A2-forward), 5′-CCC CAT AGT CTC ACA TAA CGT AGT GGG T-3′ (UGT2A2-reverse), 5′-ACC AAC TGG GAC GAC ATG GAG AAA A-3′ (β-actin-forward) and 5′-TAC GGC CAG AGG CGT ACA GGG ATA G-3′ (β-actin-reverse). The UGT2A2 primers were designed to include the predicted UGT2A2 exon 1–2 mRNA splice junction to ensure specificity for mature UGT2A2 mRNA. PCR reactions were performed in a thermal cycler (Model 9600, Applied Biosystems) as follows: 95 oC for 10 min followed by 15 cycles of 93 °C for 30 sec, a stepwise decrease in temperature from 65 °C to 50 °C for

30 sec and 72 °C for 1 min, and then 30 cycles of 93 °C for 30 sec, 50 °C for 30 sec and 72 °C for 30 sec.

Sequencing of UGT2A2 cDNA from human fetal nasal mucosa mRNA

Reverse transcribed human fetal nasal mucosa mRNA (from fetus #1, as describe above) was used to PCR amplify and sequence the predicted UGT2A2 mRNA coding region. Briefly, the PCR reaction included 1 uL of cDNA, 20 uL of Platinum *taq* HiFi PCR Supermix (Invitrogen), and 1 uL each (200 nM final concentration) of the following primers: 5′-GGA TGG TTT CCA TAA GGG ATT TTA CCA-3′ (Pri723) and 5′-AGG ACT TCC ACT ACT CAG GAT TTT GCC-3′ (Pri724). Untranscribed fetal nasal mucosa mRNA was also used as negative control. PCR reactions were performed as described above except that the extension time was increased to 1 min. PCR product was visualized on a 1.5% agarose gel with ethidium bromide staining, and sequenced by the Tufts University Core Facility (Boston, MA) after ExoSap-IT reagent treatment (USB, Cleveland, OH). Sequencing primers included Pri723 and Pri724 as well as internal primers 5′-GAC CAG ATG ACC TTT GGT GAA AGG ATT-3′ (Pri499), 5′-CCC CAT AGT CTC ACA TAA CGT AGT GGG T-3′ (Pri500). PCR reactions were performed as described below for amplification of the full length UGT2A2 cDNA except that the extension time was reduced to 30 sec.

Quantitation of UGT2A mRNA in human tissues

Real-time PCR was used to quantitate UGT2A1, UGT2A2, and UGT2A3 mRNA expression (relative to 18S rRNA expression) in the five tissues described above, as well as in adult nasal mucosa (pooled) and small intestine mucosa (pooled). Biopsies of nasal mucosa from the upper aspect of the middle turbinate of four adults (24, 38, and 40 year old females, 23 year old male) were provided by the Monell Chemical Senses Center (Philadelphia, PA) and cDNA prepared as described for fetal nasal mucosa and pooled prior to PCR. Pooled small intestine mucosa RNA samples (n = 5 white American donors) were from Ambion (USA), while lung RNA (adult male African-American) was from BD-Clontech. Real-time quantitative PCR (Model 7300, Applied Biosystems, USA) were performed with 20μL reaction volumes including Sybr Green 2X master mix (Applied Biosystems, USA), 5μL of 1:10 diluted cDNA, and 200 nM of each primer. For UGT2A1, Universal 2X master mix (Applied Biosystems, USA) was used instead of Sybr green 2X master mix, and 900 nM of the Taqman probe (FAM-5′-AGC ATA ATG TGA CTG TCC TAG TTG CCT CTG GTG CA-3′-BHQ; IDT, Coralville, Iowa) was added. In addition to the UGT2A2-forward and UGT2A2-reverse primers described above, other primer pair sequences were as follows: 5′-CCC CTC GAT GCT CTT AGC TGA GTG T-3′ (18S-rRNA-forward), 5′-CGC CGG TCC AAG AAT TTC ACC TCT-3′ (18S-rRNA-reverse), 5′-ATG AGG TAA CAG TAT TGA CTC ACT CAA AGC-3′ (UGT2A3-forward), and 5′-GTT GAT AAG CCT GGC AAG ACA TTC A-3′ (UGT2A3-reverse). Amplification specificity was ensured initially by sequencing of representative PCR products, and in each run by PCR product duplex melting temperature analysis. mRNA concentrations were calculated using standard curves of PCR threshold cycle number versus concentration of template derived from serial dilutions of purified PCR product (UGT2A3) or plasmid (UGT2A1 and UGT2A2). Curves were linear ($R^2 > 0.99$) over the concentration range 10^{-9} to 10^{-14} M for 18S rRNA and 10^{-14} to 10^{-18} M for other gene products, which defined the upper and lower quantitation limits of the respective assays. Results were expressed as the mean (± SD, N=3) number of mRNA copies per 10^9 copies of 18S rRNA.

Glucuronidation activity assays

Samples for the activity screenings contained 5–50 μg of recombinant UGT (in a microsomal preparation), 50 mM phosphate buffer pH 7.4, 10 mM $MgCl_2$, 5 mM

saccharolactone, 5 mM UDPGA, 0.4 – 10 % DMSO and 200 μM of the tested aglycone substrate, in a total volume of 100 μl. The incubation times, at 37 °C, were either 30 or 60 min, except for HDCA where the incubation time was 150 min. Both protein concentrations in the assays and incubation times were within the linear range of the different activities. The reactions were terminated by the addition of 10 μl ice cold 4 M perchloric acid and transfer to ice for 10 min. The 1-hydroxypyrene glucuronidation reactions were terminated by the addition of 20 μl of cold $ZnSo_4$ and 200 μl of MeOH, followed by 10 min cooling on ice and then sonication for 10 min. The proteins were sedimented by centrifugation at 16100 *g* and the supernatants were subjected to HPLC analyses on a Shimadzu LC-10 model (Shimadzu Corporation, Kyoto, Japan).

The HPLC conditions for 4-aminobiphenyl, estradiol, ethinylestradiol, 1-hydroxypyrene, 4-methylumbelliferone, 1-naphthol, 4-nitrophenol, scopoletin and umbelliferone were as previously described (Itäaho et al 2008, Kurkela et al 2003, Luukkanen et al 2005). Estriol glucuronides were separated with Hypersil BDS-C18 150 × 4.6 mm (Hewlett-Packard) column at 40°C, a flow rate of 1.3 ml/min in 50 mM phosphate buffer pH 3.0/MeOH, 65/35 %, and a total run time of 17 minutes. Glucuronides were detected by fluorescence using 280 nm (excitation) and 305 nm (emission). HDCA glucuronides were also separated with Hypersil BDS-C18 150 × 4.6 mm column at 40°C, but the mobile phase consisted of 10 mM NH_4Ac pH 4.5/ACN, 70/30 %, and the flow rate and total run times were 0.8 ml/min and 25 min, respectively. Detection and quantification of HDCA glucuronides was done using radioactive detection with [^{14}C]-UDPGA. The 3 different phenylphenols, 2-, 3- and 4-, were separated from the respective glucuronides using the Chromolith SpeedROD rp-18e 50 × 4.6 mm (Merck) column at 25°C with gradient flow starting at 1.5 ml/min (0–4.3 min), then 2.5 ml/min (4.3–9 min), and again 1.5 ml/min (9–10 min). The mobile phase was of 50 mM phosphate buffer pH 3.0/MeOH, 60/40 %. The detection in the case of phenylphenols was by fluorescence, at 259 nm (excitation) and 340 nm (emission).

With the exception of HDCA, ethinylestradiol and 4-phenylphenol, the glucuronides were quantified using authentic glucuronides (see Materials) as standards. HDCA, ethinylestradiol and 4-phenylphenol glucuronidation were determined using a combination of radioactive and fluorescence detection. The radiolabeled assay mixtures consisted of 25–50 μg of protein, or 200–400 μg in the case of HDCA, 50 mM phosphate buffer pH 7.4, 10 mM $MgCl_2$, 5 mM saccharolactone, 100–500 μM of the respective aglycone substrate, 50 μM cold UDPGA and 11.1 μM radiolabeled [^{14}C] UDPGA. The samples were analyzed in duplicate using the 1100 model HPLC (Agilent Technologies, Waldbronn, Germany) combined with a radiochemical detector (Model 9701, Reeve Analytical, Glasgow, U.K.). The glucuronides were quantified by the peak areas of the [^{14}C]-UDPGA-containing metabolites.

The kinetic analyses were done in triplicates, essentially as described above, but with 10–18 different aglycone concentrations for each compound (highest value with 4-phenylphenol in UGT2A1 due to unusual kinetics). In the case of 4-phenylphenol, the aglycone concentrations were between 0.2 and 1000 μM. In 4-nitrophenol kinetic assays the aglycone concentrations were between 20 and 4000 μM, and for the 4-methyl umbelliferone, the concentrations were either between 10 and 1000 μM (UGT2A1) or 10–4000 μM (UGT2A2). The final DMSO concentration in the reactions was 2–5 %. The UDPGA kinetic assays were carried out in the presence of 8 different UDPGA concentrations, between 20 and 5000 μM. The aglycone substrates in these assays were either 500 μM 4-methylumbelliferone (UGT2A1), or 750 μM 4-phenylphenol (UGT2A2). The kinetic constants were estimated by analyzing the experimental data with GraphPad Prism version 4.02 (GraphPad Software Inc., San Diego, CA).

Results

Human UGT2A1 was previously shown to be expressed in the nasal mucosa (Jedlitschky et al., 1999; Zhang et al., 2005), and here we have re-cloned the UGT2A1 cDNA using mRNA from this tissue. DNA sequencing of the newly cloned UGT2A1 revealed one difference from the original UGT2A1 sequence (NM_006798.1), namely, the nucleotide at position 275 (starting from the first ATG, equals to position 338 of the DNA sequence in Jedlitschky et al., 1999) in all our clones was T, not C as previously reported (Jedlitschky et al., 1999). At the protein level this difference translates into Leu, instead of Ser at position 92 (see GenBank accession no. CAB41974 for the older version). Our results concerning the sequence of UGT2A1 are in agreement with more recent entries to the database, such as NM_006798.2 and EAX05594. It thus appears that UGT2A1 has a leu at position 92 of the protein sequence. Hence, it is possible that a Ser at position 92 of UGT2A1 was a PCR error in the original cloning work, but the option of polymorphism could not be fully discarded at this stage.

A synthetic cDNA for UGT2A2 was constructed based on the assumption that UGT2A1 and UGT2A2 share exons 2–6 (Mackenzie et al., 2005). Exon 1 of UGT2A2 was amplified from genomic DNA and, using an Aat2 restriction site that was inserted as “silent mutation” in the 3′-end of the PCR product, very close to the border between exon 1 to exon 2, combined with exons 2–6 that were amplified from the cloned UGT2A1 and contained such an engineered Aat2 restriction site at the 5′-end of the PCR product (see Methods for details).

Several fetal and adult human tissues were examined for the presence of UGT2A2 mRNA by RT-PCR analysis, using primers that spanned the predicted UGT2A2 exon 1 to exon 2 junction. The primers were designed to ensure specific amplification of spliced mature UGT2A2 mRNA and to exclude the possibility of amplification of the UGT2A1 primary mRNA transcript. As shown in Fig. 1, UGT2A2 mRNA was detected in human fetal nasal mucosa tissues, but not in fetal lung, liver, or adult liver. Control gene (β-actin) expression was detected in all tissues analyzed, while amplification was not detected in all samples that lacked reverse transcriptase enzyme.

The entire coding region of the predicted UGT2A2 mRNA was subsequently amplified by RT-PCR using RNA derived from human fetal nasal mucosa, and then sequenced. The DNA sequence of the entire coding region of UGT2A2 that amplified from human fetal nasal mucosa (deposited in GenBank with accession number FJ664272) was identical to the synthetic UGT2A2 cDNA that we had generated, with the exception of the silent mutation (Aat2 restriction site) that was introduced during the synthetic gene construction (see Methods). It should be noted that the UGT2A2 sequence we obtained differed from the current UGT2A2 Genbank reference sequence (NM_001105677.1) in that our sequence contained an additional 24 nucleotides in the 5′ coding region (N-terminal of protein) resulting in a predicted protein size of 536 amino acids as compared with 528 amino acids for NM_001105677.

An alignment of the 3 human UGTs of subfamily 2A is shown in Fig. 2. As described above, there is an apparent disagreement between our results and the GenBank protein reference sequence entry for human UGT2A2, NP_001099147, the latter being shorter by 8 amino acids at the N-terminal end. Translation of the DNA sequence suggests that the first ATG of UGT2A2 is as shown in Fig. 2, and sequencing of the RT-PCR product from the fetal nasal mucosa (Fig. 1) confirmed that the mRNA extends at least to that first ATG. It is thus unclear to us why the protein in GenBank (NP_001099147) starts at the 2nd ATG, the 9th codon of the protein coding segment of the gene (encircled M in Fig. 2). Nevertheless, as a result of this, the position number of each amino acid in our sequence (Fig. 2) is n+8 with

respect to the sequence in NP_001099147. It may also be added here that the question which is the correct first ATG is unlikely to affect the protein sequence of the mature UGT2A2 since the signal sequence is probably cleaved off following translocation of the newly synthesized protein into the endoplasmic reticulum, as has been shown experimentally for recombinant UGT1A9 (Kurkela et al., 2003).

Using quantitative real-time PCR, comparative expression analysis was expanded to include the other UGT2A isoforms (UGT2A1 and UGT2A3) and also evaluation of other human tissues, including adult nasal mucosa, lung, liver and small intestine samples. The results (Fig. 3) showed substantial expression of both UGT2A1 and UGT2A2 in both fetal and adult nasal mucosa, although the expression levels of the two UGTs averaged 2- to 4-fold higher in fetal tissues compared with adult tissues. Furthermore, UGT2A2 levels were consistently lower (by 60 to 70%) compared with UGT2A1 levels in both adult and fetal nasal tissues. UGT2A3 was detected in much lower levels in adult nasal mucosa, but was undetectable in fetal nasal mucosa. Although UGT2A1 was not detected in any other tissue analyzed, very small amounts of UGT2A2 mRNA were found in adult lung and small intestine, as well as in fetal liver. UGT2A3 was most highly expressed in adult small intestine and liver with much lower levels in fetal liver and lung.

UGT2A1, UGT2A2 and UGT2A3 were expressed in baculovirus-infected insect cells as His-tagged proteins, containing the same C-terminal fusion peptide as the UGTs of subfamily 2B (Kurkela et al., 2003). The His-tag was used to evaluate the relative expression levels of the different recombinant UGTs in order to correct (normalize) the glucuronidation rates according to the amount of UGT in each membrane batch (see Methods for details). It may also be noted that the infection of the cells was examined in a preliminary set of experiments to avoid over-loading of the cells, a situation that may lead to the accumulation of full-length but unfolded protein that, nevertheless, reacts with the anti-His-tag antibodies. The activities of the three recombinant UGT2As were screened with several aglycone substrates, each at a single concentration. It may be noted here that the reaction conditions in this set of assays were not necessarily optimal in each case, particularly with respect to the aglycone concentration.

Similar to the results in our previous study on UGT2A3 (Court et al., 2008), in the current set of experiments UGT2A3 exhibited glucuronidating activity only towards HDCA (no other bile acids were included, Table 1). The rate of HDCA glucuronidation by UGT2A3 was rather low, 5 pmol/min/mg, but nevertheless higher than that of UGT2A1 with HDCA. The HDCA glucuronidation activity of UGT2A2 was, however, almost twice as high as the respective activity of UGT2A3 (Table 1). In addition, 3- and 4-phenylphenols turned out to be good substrates for UGT2A2. The latter compounds were tested since in the earlier study on UGT2A1, 3-phenylphenol as appeared to be the best substrate (Jedlitschky et al., 1999). Unfortunately, it was difficult to obtain a highly pure sample of 3-phenylphenol, so for the kinetic assays shown below we have selected 4-phenylphenol, another good substrate for UGT2A2 and, especially, for UGT2A1 (Table 1 and Jedlitschky et al., 1999).

A comparison of the glucuronidation rates of UGT2A1 and UGT2A2 towards the 3 different phenylphenols suggests that the substrate specificity and regioselectivity of UGT2A2 is nearly identical to that of UGT2A1 except that the turnover rate of UGT2A2 was about 6 fold lower than UGT2A1 (Table 1). It is thus interesting that the results with the 3 estrogens, estriol, estradiol and ethinylestradiol, revealed a significantly different situation with respect to regioselectivity. UGT2A1 exhibited a clear preference for the 17-OH (17-OH or 16-OH in the case of estriol) of the tested estrogens. For ethinylestradiol the only target hydroxyl is the 3-OH and UGT2A1 was practically inactive in the glucuronidation of this estrogen

derivative. For UGT2A2, however, ethinylestradiol was the best substrate among these three steroids.

On the other hand, UGT2A2 was nearly inactive in estriol glucuronidation and did not yield any detectable estradiol 17-glucuronide. Nevertheless, UGT2A2 catalyzed estradiol glucuronidation at the 3-OH at about the same low rate as UGT2A1 (Table 1).

The activity screening results also revealed that the UGT2A1 catalyze the glucuronidation of 1-naphthol, 4-methylumbelliferone and 1-hydroxypyrene at much higher rates than the respective activity for UGT2A2 under the conditions used in these experiments. Large differences between the activity of UGT2A1 and UGT2A2 towards other substrates, such as 4-phenylphenol, umbelliferone, and 4-nitrophenol were also observed (Table 1).

In order to determine whether the large differences in glucuronidation rates between UGT2A1 and UGT2A2 arise mainly from low substrate affinity or from limited turnover rate in UGT2A2, we have examined the enzyme kinetics of 4-phenylphenol, 4-methylumbelliferone, and 4-nitrophenol glucuronidation. The glucuronidation of 4-nitrophenol by UGT2A1 followed Michaelis-Menten kinetics, whereas 4-methylumbelliferone glucuronidation exhibited Michaelis-Menten kinetics with substrate inhibition (Fig. 4). Interestingly, the glucuronidation of 4-phenylphenol by UGT2A1 (Fig. 4A) clearly deviated from either Michaelis-Menten or sigmoidal kinetics (see below). The kinetics of 4-nitrophenol, 4-phenylphenol and 4-methylumbelliferone by UGT2A2 followed Michaelis-Menten kinetics (Fig. 5). We have also examined the UDPGA K_m in both UGT2A1 and UGT2A2, using 4-methylumbelliferone or 4-phenylphenol as the aglycone substrate for UGT2A1 and UGT2A2, respectively (Figs. 4 and 5). The results indicated that the affinity for the co-substrate, UDPGA, in UGT2A1 and UGT2A2 is similar.

The glucuronidation of 4-phenylphenol by UGT2A1 exhibited an unusual kinetics that is best described by a two-sites model, assuming two different substrate binding site that vary largely in affinity. This interpretation also implies that the K_m for 4-phenylphenol at the high-affinity site, about 1 μM, is by far the lowest K_m value that was observed in the current study. In order to better demonstrate the basis for suggesting two-sites as the kinetic model for the glucuronidation of 4-phenylphenol by UGT2A1, the results of this kinetic assay are also presented as an Eadie-Hofstee plot (Fig. 6).

The enzyme kinetic constants are listed in Table 2. They clearly show that for the 3 different aglycone substrates that were included in these assays, the affinity of UGT2A1 for the substrate is much higher than in UGT2A2. The K_m values for the aglycone in UGT2A1 were over 100 fold smaller than the respective K_m values in UGT2A2 (Table 2). In the case of 4-phenylphenol, the substrate for which UGT2A1 exhibited two-site kinetics (Figs. 4 and 6, Table 2), UGT2A2 followed Michaelis-Menten kinetics, exhibiting a single K_m value that was much closer to the apparent low-affinity site in UGT2A1 that the high affinity one (Table 2). These differences, as well as some similarities, in the activity of these two highly homologous proteins (Fig. 2) are likely to become useful when trying to identify specific amino acids that are responsible for the binding of different compounds.

Discussion

Of the 19 human UGTs of subfamilies 1A, 2A and 2B, 18 have already been shown to be expressed in one or more human tissue (Jedlitschky et al., 1999; Tukey and Strassburg, 2001; Lévesque et al., 2001; Turgeon et al., 2001; Mackenzie et al., 2005; Finel et al., 2005; Court et al., 2008; Nakamura et al., 2008; Ohno and Nakajin, 2009). The 19th UGT, the “missing” UGT2A2, has never been functionally characterized. There is one report on its expression in the gastrointestinal tract (Tukey and Strassburg, 2001), but it only concerns

exon 1 and lacks experimental details to show that full-length UGT2A2 was detected. Moreover, the expression of UGT2A2 as a full-length enzyme was uncertain since the exons encoding its C-terminal half have never been identified. Exon sharing governs the expression of all the UGTs of subfamily 1A (Owens et al., 2005), but it was not earlier observed in UGTs of family 2. As far as was known by 2005, UGT2A1 and all the UGTs of subfamily 2B were encoded by separate genes, each including all the 6 exons for the respective proteins. The subsequent characterization of UGT2A3 was in full agreement with this since the gene encoding this enzyme, too, contained 6 exons (Court et al., 2008). Nevertheless, Mackenzie and coauthors had previously suggested that UGTs 2A1 and 2A2 shared exons 2–6, thereby allowing for the expression of full-length UGT2A2 (Mackenzie et al., 2005).

Following works on UGT1A5 (Finel et al., 2005) and UGT2A3 (Court et al., 2008), two human UGTs that were earlier assumed not to be expressed at all, or were simply overlooked, we were interested to find out if UGT2A2, is expressed as well. In addition, knowing that UGT2A1 is perhaps the human UGT that can catalyze the glucuronidation of a large number of different aglycones, at a considerable rate (Jedlitschky et al., 1999; Sten et al., 2009), while UGT2A3 was among the UGTs with most narrow substrate selectivity, it was interesting to examine the activities of UGT2A2, the last member of subfamily UGT2A. It was hoped, and still hoped, that characterizing the activities of UGT2A2 will provide new information that, sooner or later, will be important in solving the large “puzzle” of the relation between protein sequence and substrate selectivity among all the human UGTs. Hence, we embarked on producing the human UGT2A2, assuming that the suggestion of exon sharing with UGT2A1 is correct. In parallel, we set out to test this suggestion and try to find out in which human tissues UGT2A2 is expressed.

Our results clearly show that UGT2A2 is expressed in the nasal mucosa (Figs. 1 and 3). This means that UGT2A2 does not only share exons 2–6 with UGT2A1, it also shares with it a similar tissue expression pattern (Fig. 3). Both UGTs are primarily expressed in nasal epithelium, at least based on screening of a number of tissues known to express a large number and variety of UGTs, including liver and intestines. In the case of UGT2A2 we have detected trace amounts of mRNA also in three other tissues, while UGT2A1 was only found in the nasal mucosa (Fig. 3). The 3rd member of UGT2A subfamily, UGT2A3 exhibited a strikingly different tissue expression pattern in that it was mainly found in the liver and small intestine (Fig. 3), in full agreement with the previous study on this enzyme (Court et al., 2008).

Another interesting feature in the gene expression of UGT2A1 and UGT2A2 was their higher expression level in fetal nasal mucosa relative to adult nasal mucosa (Fig. 3). The fetal nasal mRNA samples were only from two individuals and, hence, no clear conclusion about possible developmental regulation of these genes can be drawn at this stage. Nevertheless, the clear finding that these enzymes are expressed in the fetus is interesting with respect to the possible role of active UGTs in the nasal epithelium. It was previously suggested that an important role for UGT2A1 (then termed “UGT-olf”) in this tissue is termination of olfactory signals (Lazard et al., 1991;Jedlitschky et al., 1999). However, our observation that UGT2A1, as well as UGT2A2, are highly expressed in fetal nasal epithelium (Fig. 3), may render the role of olfactory signal termination less likely. Detoxification of potentially toxic waste compounds in the amniotic fluid before birth, and air-born chemical after birth, might be a better description of the physiological roles of both UGT2A1 and UGT2A2. It is also worth pointing out that alongside UGT2A1 and UGT2A2, several cytochrome P450 enzymes are more highly expressed in fetal nasal epithelium as compared with adult nasal epithelium (Chen et al., 2003).

UGT2A1 has a verybroad substrate specificity, a property that was already noticed in the first study on this enzyme (Jedlitschky et al., 1999). Our current findings further extend the list of aglycones that can be conjugated by UGT2A1 (Table 1), and recent studies from our laboratory that were carried out using the same batches of recombinant UGTs 2A1–2A3, add more compounds to this list (Itäaho et al., 2008; Sten et al., 2009). The kinetic assays in the present work, particularly with 4-phenylphenol as the aglycone substrate, reveal a new dimension to the substrate specificity of UGT2A1, the apparent presence of both a high affinity and a low affinity binding sites (Fig. 6). The kinetic analysis of 4-phenylphenol glucuronidation by UGT2A1 neither reveals allosteric interactions between the two sites, nor provides an indication for an auto-activation phenomenon (Figs. 4A and 6). If such a kinetic curve would have been observed in microsomes from a given human tissue, it could be argued that the substrate is glucuronidated by two different enzymes that vary largely in their substrate affinity. However, since we have worked with a recombinant UGT2A1, both the low and the high affinity sites are likely from the same enzyme. It might be argued that the observed kinetics is an artifactual outcome of the expression system, but it should be noted in this respect that such a two-site kinetics was not observed for UGT2A1 glucuronidating 4-methylumbelliferone or 4-nitrophenol (Fig. 4).

It may be added here that two-site kinetics was previously reported for the glucuronidation of morphine by UGT2B7, at either the 3-OH or the 6-OH (Stone et al., 2003). In a recent study it was suggested that UGT2B7 has two substrate binding sites and at least one effector site, and that their affinity for the substrate may depend on the particular compound, as well as on not fully understood factors (Uchaipichat et al., 2008).

UGT2A2 also exhibited a broad substrate selectivity, but its glucuronidation rates in most cases were much lower than UGT2A1. However, the results of the screening assays (Table 1) may underestimate the ability of UGT2A2 to reach high turnover rates since, as subsequently revealed by the kinetic assays, its affinity for the aglycone substrates is often low. The enzyme kinetic analyses (Fig. 5, Table 2) indicated that while the K_m of UGT2A2 for the 3 tested substrates were much higher than the corresponding values in UGT2A1, the differences in V_{max} values between the two enzymes were not as large (Table 2). Since the main differences between these two highly homologous enzymes are in the K_m values, UGT2A1 and UGT2A2 might provide a good platform to explore the interactions of aglycone substrates with the binding sites of different UGTs.

Alongside the similarity in substrate selectivity between UGT2A1 and UGT2A2, there were also differences between them in this respect. Perhaps the most remarkable difference was in the glucuronidation of ethinylestradiol, a synthetic estrogen in which a bulky ethinyl group attached to carbon 17 of the estrogen and sterically hindering conjugation at the 17-OH. Interestingly, for UGT2A2 the presence of the ethinyl group at C17 significantly enhanced glucuronidation at the other side of the steroid molecule, at the 3-OH position. It remains to be elucidated what leads to this difference between the two enzymes, and whether or not it is linked to the failure of UGT2A2 to catalyze detectable rates of estriol-3-glucuronide formation (Table 1).

In summary, we have cloned, expressed and characterized UGT2A2, as well as further studied UGT2A1 and UGT2A3. The results revealed that UGT2A2 is a functional enzyme, that there is exon sharing between UGT2A1 and UGT2A2, and that both of them are mainly expressed in human nasal mucosa. UGT2A3 differed from UGT2A1 and UGT2A2 in nearly every aspect examined in this study. The current findings provide new leads for understanding both expression regulation and substrate selectivity of the UGTs, two important challenges in this research field.

Acknowledgments

We thank Johanna Mosorin for superb technical assistance, as well as Dr. Leah M. Hesse and Qin Hao for help with the qRT-PCR analyses. We thank Dr. Alan Fantel of the Birth Defect Research Laboratory at the University of Washington (funded by NIH Grant HD00836) for providing human tissues.

Sponsorship: Sigrid Juselius foundation (MF), National Institutes of Health (GM61834 to MHC and ES07462 to XD). Adult nasal tissues acquisition was supported by NIH-NIDCD P50 006760 (to KKY and PD). The content is solely the responsibility of the authors and does not necessarily represent the official views of the National Institutes of Health.

Abbreviations

HDCA	hyodeoxycholic acid
UDPGA	UDP-glucuronic acid
UGT	UDP-glucuronosyltransferase

References

Bélanger A, Hum DW, Beaulieu M, Lévesque E, Guillemette C, Tchernof A, Bélanger G, Turgeon D, Dubois S. Characterization and regulation of UDP-glucuronosyltransferases in steroid target tissues. J Steroid Biochem Mol Biol. 1998; 65:301–310. [PubMed: 9699884]

Buckley DB, Klaassen CD. Tissue- and gender-specific mRNA expression of UDP-glucuronosyltransferases (UGTs) in mice. Drug Metab Dispos. 2007; 35:121–127. [PubMed: 17050650]

Chen Y, Liu YQ, Su T, Ren X, Shi L, Liu D, Gu J, Zhang QY, Ding X. Immunoblot analysis and immunohistochemical characterization of CYP2A expression in human olfactory mucosa. Biochem Pharmacol. 2003; 66:1245–1251. [PubMed: 14505803]

Court MH, Hazarika S, Krishnaswamy S, Finel M, Williams JA. Novel polymorphic human UDP-glucuronosyltransferase 2A3: cloning, functional characterization of enzyme variants, comparative tissue expression, and gene induction. Mol Pharmacol. 2008; 74:744–754. [PubMed: 18523138]

Finel M, Kurkela M. The UDP-glucuronosyltransferases as oligomeric enzymes. Curr Drug Metab. 2008; 9:70–76. [PubMed: 18220573]

Finel M, Li X, Gardner-Stephen D, Bratton S, Mackenzie PI, Radominska-Pandya A. Human UDP-glucuronosyltransferase 1A5: identification, expression and activity. J Pharmacol Exper Ther. 2005; 315:1143–1149. [PubMed: 16120810]

Gong QH, Cho JW, Huang T, Potter C, Gholami N, Basu NK, Kubota S, Carvalho S, Pennington MW, Owens IS, Popescu NC. Thirteen UDPglucuronosyltransferase genes are encoded at the human UGT1 gene complex locus. Pharmacogenetics. 2001; 11:357–368. [PubMed: 11434514]

Heydel J, Leclerc S, Bernard P, Pelczar H, Gradinaru D, Magdalou J, Minn A, Artur Y, Goudonnet H. Rat olfactory bulb and epithelium UDP-glucuronosyltransferase 2A1 (UGT2A1) expression: in situ mRNA localization and quantitative analysis. Brain Res Mol Brain Res. 2001; 90:83–92. [PubMed: 11376859]

Itäaho K, Mackenzie PI, Ikushiro S, Miners JO, Finel M. The configuration of the 17-hydroxy group variably influences the glucuronidation of beta-estradiol and epiestradiol by human UDP-glucuronosyltransferases. Drug Metab Dispos. 2008; 36:2307–2315. [PubMed: 18719240]

Jedlitschky G, Cassidy AJ, Sales M, Pratt N, Burchell B. Cloning and characterization of a novel human olfactory UDP-glucuronosyltransferase. Biochem J. 1999; 340:837–843. [PubMed: 10359671]

King CD, Rios GR, Green MD, Tephly TR. UDP-glucuronosyltransferases. Curr Drug Metab. 2000; 1:143–161. [PubMed: 11465080]

Kurkela M, García-Horsman JA, Luukkanen L, Mörsky S, Taskinen J, Baumann M, Kostiainen R, Hirvonen J, Finel M. Expression and characterization of recombinant human UDP-glucuronosyltransferases (UGTs). UGT1A9 is more resistant to detergent inhibition than other

UGTs and was purified as an active dimeric enzyme. J Biol Chem. 2003; 278:3536–3544. [PubMed: 12435745]

Kurkela M, Hirvonen J, Kostiainen R, Finel M. The interactions between the N-terminal and C-terminal domains of the human UDP-glucuronosyltransferases are partly isoform-specific, and may involve both monomers. Biochem Pharmacol. 2004; 68:2443–2450. [PubMed: 15548391]

Kurkela M, Patana AS, Mackenzie PI, Court MH, Tate CG, Hirvonen J, Goldman A, Finel M. Interactions with other human UDP-glucuronosyltransferases attenuate the consequences of the Y485D mutation on the activity and substrate affinity of UGT1A6. Pharmacogenet Genomics. 2007; 17:115–126. [PubMed: 17301691]

Lazard D, Zupko K, Poria Y, Nef P, Lazarovits J, Horn S, Khen M, Lancet D. Odorant signal termination by olfactory UDP glucuronosyl transferase. Nature. 1991; 349:790–793. [PubMed: 1900353]

Lévesque E, Turgeon D, Carrier JS, Montminy V, Beaulieu M, Bélanger A. Isolation and characterization of the UGT2B28 cDNA encoding a novel human steroid conjugating UDP-glucuronosyltransferase. Biochemistry. 2001; 40:3869–3881. [PubMed: 11300766]

Luukkanen L, Mikkola J, Forsman T, Taavitsainen P, Taskinen J, Elovaara E. Glucuronidation of 1-hydroxypyrene by human liver microsomes and human UDP-glucuronosyltransferases UGT1A6, UGT1A7, and UGT1A9: development of a high-sensitivity glucuronidation assay for human tissue. Drug Metab Dispos. 2001; 29:1096–1101. [PubMed: 11454727]

Luukkanen L, Taskinen J, Kurkela M, Kostiainen R, Hirvonen J, Finel M. Kinetic characterization of the 1A subfamily of recombinant human UDP-glucuronosyltransferases. Drug Metab Dispos. 2005; 33:1017–1026. [PubMed: 15802387]

Mackenzie PI, Bock KW, Burchell B, Guillemette C, Ikushiro S, Iyanagi T, Miners JO, Owens IS, Nebert DW. Nomenclature update for the mammalian UDP glycosyltransferase (UGT) gene superfamily. Pharmacogenet. 2005; 15:677–685.

Mackenzie PI, Rogers A, Treloar J, Jorgensen BR, Miners JO, Meech R. Identification of UDP glycosyltransferase 3A1 as a UDP N-acetylglucosaminyltransferase. J Biol Chem. 2008; 283:36205–36210. [PubMed: 18981171]

Nakamura A, Nakajima M, Yamanaka H, Fujiwara R, Yokoi T. Expression of UGT1A and UGT2B mRNA in human normal tissues and various cell lines. Drug Metab Dispos. 2008; 36:1461–1464. [PubMed: 18480185]

Ohno S, Nakajin S. Determination of mRNA expression of human UDP-glucuronosyltransferases and application for localization in various human tissues by real-time reverse transcriptase-polymerase chain reaction. Drug Metab Dispos. 2009; 37:32–40. [PubMed: 18838504]

Ouzzine M, Barré L, Netter P, Magdalou J, Fournel-Gigleux S. The human UDP-glucuronosyltransferases: structural aspects and drug glucuronidation. Drug Metab Rev. 2003; 35:287–303. [PubMed: 14705862]

Owens IS, Basu NK, Banerjee R. UDP-glucuronosyltransferases: gene structures of UGT1 and UGT2 families. Methods Enzymol. 2005; 400:1–22. [PubMed: 16399340]

Rowland A, Gaganis P, Elliot DJ, Mackenzie PI, Knights KM, Miners JO. Binding of inhibitory fatty acids is responsible for the enhancement of UDP-glucuronosyltransferase 2B7 activity by albumin: implications for in vitro-in vivo extrapolation. J Pharmacol Exp Ther. 2007; 321:137–147. [PubMed: 17237258]

Somers GI, Lindsay N, Lowdon BM, Jones AE, Freathy C, Ho S, Woodrooffe AJ, Bayliss MK, Manchee GR. A comparison of the expression and metabolizing activities of phase I and II enzymes in freshly isolated human lung parenchymal cells and cryopreserved human hepatocytes. Drug Metab Dispos. 2007; 35:1797–1805. [PubMed: 17627976]

Sten T, Bichlmaier I, Kuuranne T, Leinonen A, Yli-Kauhaluoma J, Finel M. UGT2B7 and UGT2B17 display converse specificity in testosterone and epitestosterone glucuronidation, whereas UGT2A1 conjugates both androgens similarly. Drug Metab Dispos. 2009; 37:417–423. [PubMed: 19022937]

Stone AN, Mackenzie PI, Galetin A, Houston JB, Miners JO. Isoform selectivity and kinetics of morphine 3- and 6-glucuronidation by human udp-glucuronosyltransferases: evidence for atypical

glucuronidation kinetics by UGT2B7. Drug Metab Dispos. 2003; 31:1086–1089. [PubMed: 12920162]

Strausberg RL, et al. Generation and initial analysis of more than 15,000 full-length human and mouse cDNA sequences. Proc Natl Acad Sci U S A. 2002; 99:16899–16903. [PubMed: 12477932]

Thum T, Erpenbeck VJ, Moeller J, Hohlfeld JM, Krug N, Borlak J. Expression of xenobiotic metabolizing enzymes in different lung compartments of smokers and nonsmokers. Environ Health Perspect. 2006; 114:1655–1661. [PubMed: 17107849]

Tukey RH, Strassburg CP. Human UDP-glucuronosyltransferases: metabolism, expression, and disease. Annu Rev Pharmacol Toxicol. 2000; 40:581–616. [PubMed: 10836148]

Tukey RH, Strassburg CP. Genetic multiplicity of the human UDP-glucuronosyltransferases and regulation in the gastrointestinal tract. Mol Pharmacol. 2001; 59:405–414. [PubMed: 11179432]

Turgeon D, Carrier JS, Lévesque E, Hum DW, Bélanger A. Relative enzymatic activity, protein stability, and tissue distribution of human steroid-metabolizing UGT2B subfamily members. Endocrinology. 2001; 142:778–787. [PubMed: 11159850]

Uchaipichat V, Galetin A, Houston JB, Mackenzie PI, Williams JA, Miners JO. Kinetic modeling of the interactions between 4-methylumbelliferone, 1-naphthol, and zidovudine glucuronidation by udp-glucuronosyltransferase 2B7 (UGT2B7) provides evidence for multiple substrate binding and effector sites. Mol Pharmacol. 2008; 74:1152–1162. [PubMed: 18647858]

Wells PG, Mackenzie PI, Chowdhury JR, Guillemette C, Gregory PA, Ishii Y, Hansen AJ, Kessler FK, Kim PM, Chowdhury NR, Ritter JK. Glucuronidation and the UDP-glucuronosyltransferases in health and disease. Drug Metab Dispos. 2004; 32:281–290. [PubMed: 14977861]

Zhang X, Zhang Q-Y, Liu D, Su T, Weng Y, Ling G, Chen Y, Gu J, Schilling B, Ding X. Expression of cytochrome P450 and other biotransformation genes in fetal and adult human nasal mucosa. Drug Metab Dispos. 2005; 33:1423–1428. [PubMed: 16014766]

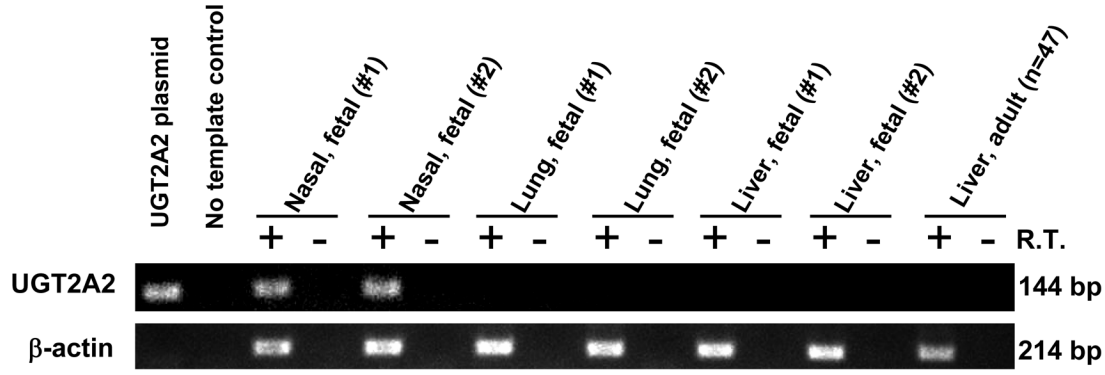

Figure 1.

Identification of UGT2A2 mRNA in human fetal nasal mucosa. PCR (45 cycles) was performed using reverse transcribed mRNA from human fetal nasal mucosa, lung, and liver (2 fetuses each) and from human adult liver (pooled from 47 donors). Primers were designed to be specific for human UGT2A2 and β-actin. PCR products were run on a 2% agarose gel and visualized by ethidium bromide staining. Expected product sizes were 144 bp (UGT2A2) and 214 bp (β-actin).

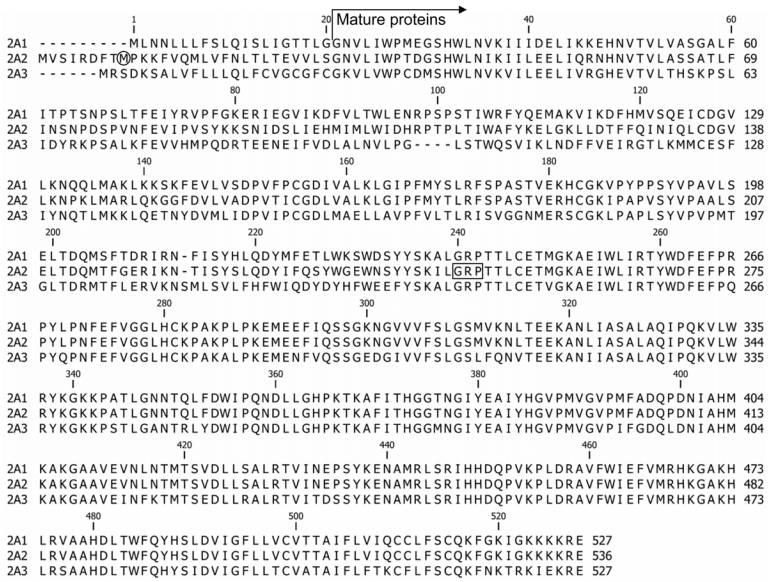

Figure 2.

Sequence alignment of the human UGTs 2A1, 2A2 and 2A3. The starting point of the mature proteins is indicated. The Met residue that is encircled near the start of UGT2A2 might be the first Met (see text for details). The boxed GRP residues in the middle of the UGT2A2 sequence indicate the position of the Aat2 restriction site that was generated in order to combine the amplified exon 1 of UGT2A2 with the cloned exons 2–6 of UGT2A1. The numbers above the sequences are according to UGT2A1.

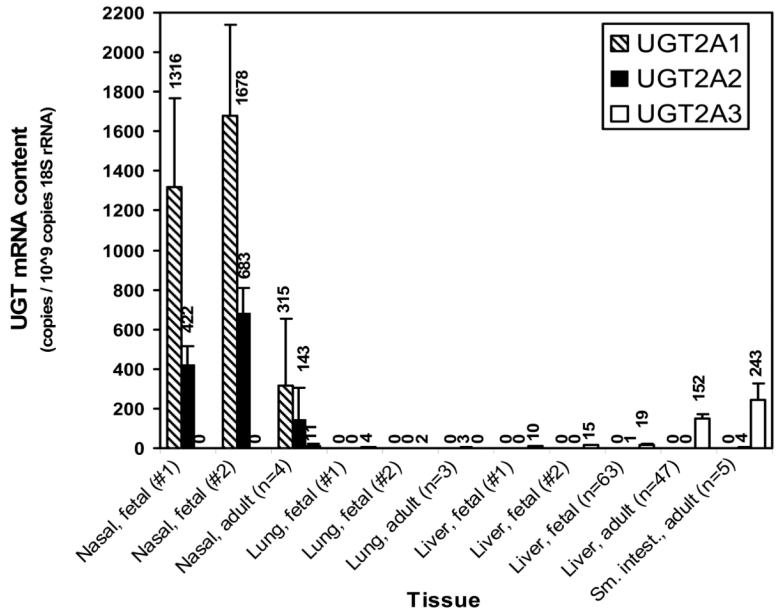

Figure 3.

Expression of UGT2A1, UGT2A2 and UGT2A3 isoform mRNA in human tissues. Quantitative real-time PCR was performed using reverse transcribed mRNA prepared from human fetal nasal mucosa (2 individuals), lung (2 individuals), and liver (2 individuals and 63 pooled donors) and also from adult lung (3 pooled donors), liver (47 pooled donors), and small intestine (5 pooled individuals). Results, mean ± SD of triplicate determinations, were normalized to 18S rRNA content.

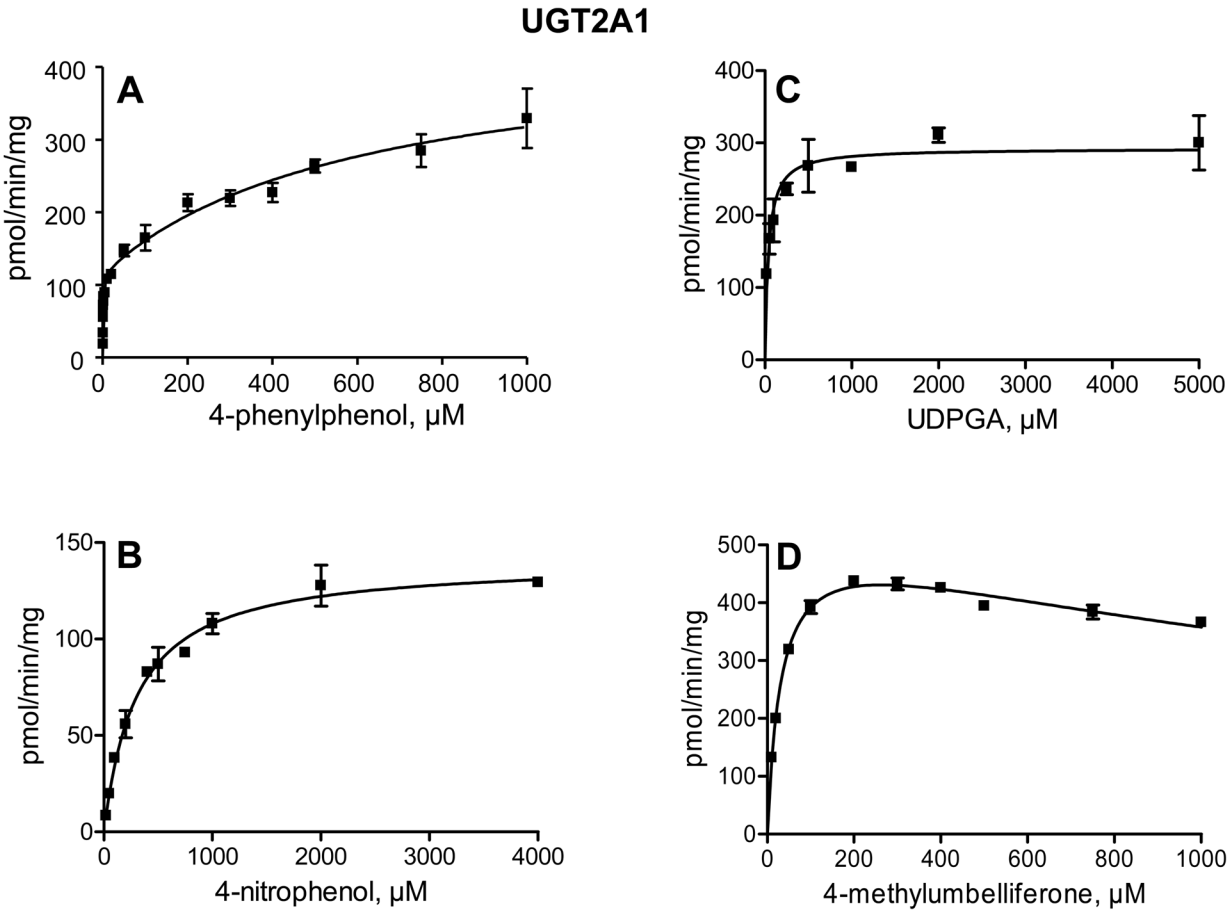

Figure 4.

Kinetics of 4-phenylphenol (A), 4-methylumbelliferone (B), and 4-nitrophenol (D) glucuronidation by UGT2A1. The aglycone substrate in the kinetic analysis for UDPGA (C) was 500 μM 4-methylumbelliferone. The analyses were done in triplicates and the SD error bars are presented.

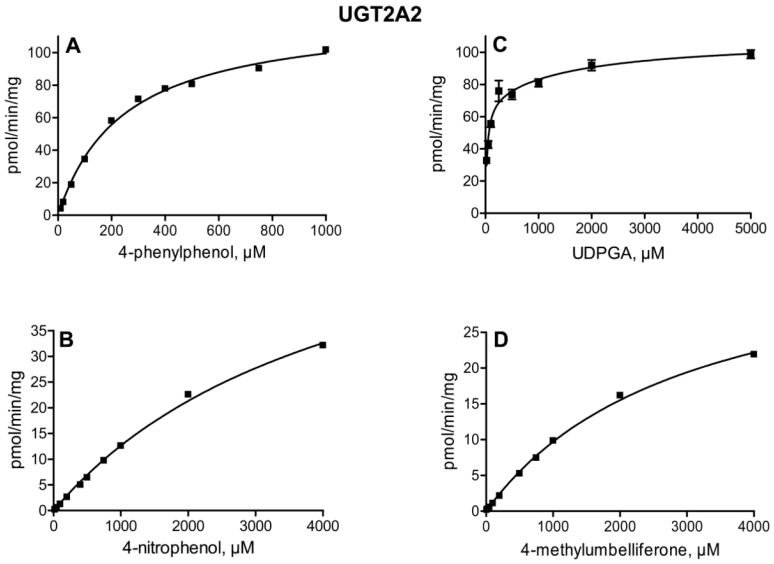

Figure 5.

Kinetics of 4-phenylphenol (A), 4-methylumbelliferone (B), and 4-nitrophenol (D) glucuronidation by UGT2A2. The aglycone substrate in the kinetic analysis for UDPGA (C) was 750 μM 4-phenylphenol. The analyses were done in triplicates and the SD error bars are presented (even if they are not easily visible in panels A, B, and D, due to very small differences between the triplicate determinations).

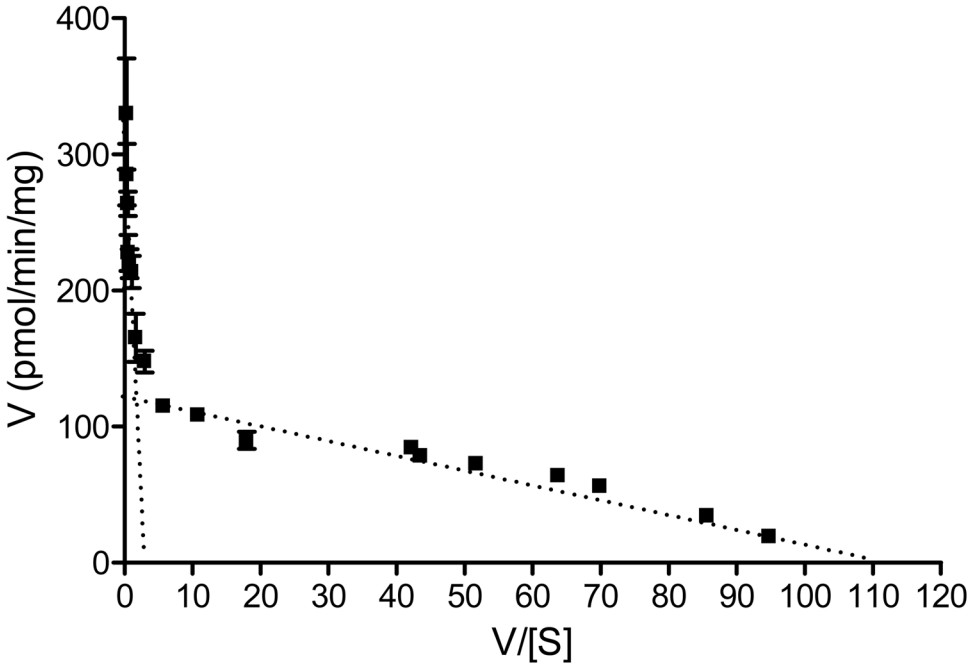

Figure 6.
An Eadie-Hofstee plot of the kinetics of 4-phenylphenol glucuronidation by UGT2A1. The data points are the same as in panel A of Fig. 4.

Table 1

Glucuronidation activities of UGT2A1, UGT2A2 and UGT2A3. Glucuronide formation rates, expressed as mean ± SD (pmol/min/mg), were corrected according to relative expression level of each enzyme (1.0 for UGT2A1, 2.1 in UGT2A2 and 0.12 for UGT2A3, see Methods for details). The concentration of the aglycone substrates was 200 μM. nd: no glucuronides detected.

	UGT2A1	UGT2A2	UGT2A3
4-aminobiphenyl	nd	nd	nd
Estradiol (3- glucuronide)	0.70 ± 0.03	1.50 ± 0.03	nd
Estradiol (17- glucuronide)	2.2 ± 0.1	< 0.1	nd
Estriol (3- glucuronide)	nd	nd	nd
Estriol (16 or 17- glucuronide)	14.1 ± 0.5	0.10 ± 0.03	nd
Ethinylestradiol	< 0.1	9.5 ± 0.5	nd
1-hydroxypyrene	198 ± 2	5.3 ± 0.1	nd
Hyodeoxycholic acid (HDCA)	2.1 ± 0.1	8.1 ± 0.5	4.9 ± 0.4
4-methylumbelliferone	548 ± 40	2.9 ± 0.1	nd
1-naphtol	314 ± 24	4.1 ± 0.1	nd
4-nitrophenol	60.1 ± 4	3.6 ± 0. 1	nd
2-phenylphenol	15.7 ± 0.6	1.3 ± 0. 1	nd
3-phenylphenol	339 ± 6	62 ± 1	nd
4-phenylphenol	249 ± 22	74 ± 2	nd
Scopoletin	283 ± 12	7.7 ± 0.1	nd
Umbelliferone	233 ± 10	0.60 ± 0.03	nd

Table 2

Enzyme kinetic constants for the glucuronidation of 4-nitrophenol, 4-methylumbelliferone and 4-phenylphenol by recombinant UGT2A1 and UGT2A2 (see Figs. 4, 5 for the enzyme kinetic plots). The K_m and V_{max} (pmol/min/mg) values represent means ± S.D. from triplicate incubations.

	UDPGA*		4-nitrophenol		4-methyl-umbelliferone		4-phenylphenol	
	K_m, μM	V_{max}	K_m, μM	V_{max}	K_m, μM	V_{max}	K_m, μM	V_{max}
UGT2A1	39.5 ± 8.9	292 ± 12	303 ± 35	141 ± 5	32.3 ± 2.2 K_i μMK 2135 ± 240	537 ± 13	0.9 ± 0.3 (K_m 1) 614 ± 221 (K_m 2)	116 ± 10 (V_{max} 1) 325 ± 49 (V_{max} 2)
UGT2A2	55.1 ± 7.7	91.4 ± 3	4469 ± 295	69 ± 3	2998 ± 123	39 ± 0.9	245 ± 12	124 ± 2

* The aglycone substrates for the kinetic assays with UDPGA were either 500 μM 4-methyl-umbelliferone (UGT2A1), or 750 μM 4-phenylphenol (UGT2A2).